Ultrasonic Detection of Fretting Fatigue Damage at Bolt Joints of Aluminum Alloy Plates

Sanat Wagle*and Hiroshi Kato*

* Graduate School of Science and Engineering, Saitama University, 255, Shimo-Okubo, Sakura-Ku, Saitama, 338-8570, Japan

Corresponding author:

Sanat Wagle
Graduate School of Science and Engineering
Saitama University
255, Shimo-Okubo, Sakura-Ku
Saitama, 338-8570
Japan
e-mail: sanat@hotmail.com
Tel: +81 48 858 9203 Fax: +81 48 856 2577

Abstract

The fatigue failure evaluation was carried out to determine the effect of the tightening torque of the bolt on the failure mode and the fatigue life of bolted joints of aluminum alloy plates 2024-T3 at different levels of the stress amplitude. These results were shown in the tightening torque and fatigue life diagram. Regardless the stress amplitude, when the tightening torque is relatively lower the mechanical fatigue failure occurred at the edge of the bolt hole, and the fatigue life increased with the tightening torque. When the tightening torque is increased further, the fretting wear failure occurred near the bolt hole due to the gross sliding of the specimen surface, and the fatigue life increased with the increase in tightening torque. At a higher range of tightening torque, the fatigue life decreased with the increasing tightening torque, and the fretting fatigue failure occurred near the bolt hole. A tightening torque boundary between the fretting failure and the mechanical fatigue increased with increasing stress amplitude. The ultrasonic measurement with surface acoustic wave was also carried out during the fatigue testing, and the echo reflected from the fretting fatigue crack was detected at a position 1.8~2.1 mm ahead of the bolt hole in the fastened condition.

Key Word: Nondestructive testing, Ultrasonic measurement, Aluminum alloy, Fretting, Fatigue testing, Bolt joint

1. Introduction

In machinery such as aircrafts and vehicles, structural parts are often fastened with bolts and rivets to withstand higher levels of structural loads. Since bolted and riveted parts are stress raisers due to geometrical discontinuities at holes, fatigue cracks often initiate at riveted and bolted joints to result in unexpected failures. The fatigue damage at the joints are often considered as multiple site damage (MSD) because of their multiple crack initiation sites [1] ~ [2]; the fatigue crack initiates mainly due to the high stress concentration at a hole edge [3], and the fretting also occurs at mating interfaces of the joint part due to repeated relative movement [4] ~ [5]. Fretted regions are highly sensitive to repeated loadings and lead to nucleation of cracks even at lower stresses. From these situations, many studies [4] ~ [17] have been carried out on the fretting damage, but no quantitative evaluation and analysis were performed on the effect of tightening conditions on the life cycle in consideration of the failure mode: the mechanical fatigue failure and the fretting fatigue failure.

Moreover, the crack is not visible at an early stage of the fatigue process in the bolted joints since crack initiation sites are hidden by the bolt head and the nut. The information about the crack initiation and propagation is often obtained by non-destructive methods, such as the ultrasonic measurement. Osegueda et. al. [18] and Chan and Mal [19] detected cracks at the rivet hole in plates using Lamb wave. Although small fatigue cracks can be detected by the Lamb wave from its scattering behavior, the Lamb wave method still has limitations such as the dispersive nature of the wave and presence of mixed modes with various frequencies. Therefore, the quantitative evaluation of the crack is not so easy due to difficulties in identifying individual modes existing in the reflected wave. Practically, cracks appeared at the joints have been detected by the angle beam method. In this method, the ultrasonic wave is incident on the material surface by the angle incidence, propagates inside the material, reflects from the bottom of the material, and then is irradiated to the fatigue crack. Mi et. al. [20] ~ [21] and Chiou et. al. [22] had focused their analyses on detection of the crack originated from the fastener hole by using shear wave angle beam transducers. Saka et. al. [23] ~ [26] also detected the vertical fatigue crack originated at the opposite surface of the material by using various shear wave angles. Limitation of the angle beam method also includes dispersive nature and multiple reflections of mixed modes. The scattered surface acoustic wave had been used for detection of the surface crack and the corrosion fatigue crack because of a simple path and hence of easy identification of the crack

[27] ~ [29]. However, there have been no reports on the analysis of the surface acoustic wave (SAW) to detect and to evaluate a fatigue crack at the bolted joints under fastened conditions.

The objective of this study consists of two issues. First is clarification of the influence of the tightening torque on the fatigue behavior of the bolted specimens of the aluminum alloy plate Al2024-T3: the fatigue life and the failure mode at different stress amplitudes. Second is the development of the non-destructive detection method of the fatigue crack initiated in bolted specimen under fastened conditions by using the SAW.

2. Experimental Procedure

2.1 Preparation of specimens

Specimens were fabricated from A2024-T3 (nominal chemical composition of Al-4.4 mass % Cu-0.6 mass % Mn-1.5 mass % Mg). The T3 condition consists of the solution heat treatment, the cold working and the natural aging. Nominal mechanical properties of the aluminum 2024- T3 alloy are 330 MPa in yield strength (0.2 % offset proof stress), 465 MPa in tensile strength, and 20 % in elongation to fracture in the rolling direction. Figure 1 shows the shape and dimensions of specimens for fatigue testing fabricated from A2024-T3 plate of 4 mm in thickness. In the figure, the specimen A has a bolt hole of 6.03 mm in diameter, and hereafter referred to as a bolt hole specimen, and the specimen B has a bolt joint, and hereafter referred to as a bolted specimen. A distance of the bolt hole from the specimen edge was kept twice the diameter of the hole in order to prevent the tear out of the specimen from the hole edge. Bolted specimens were fabricated by fastening two bolt hole specimens with a screw of 12.9 high grade chromium molybdenum steel (5.95 mm in diameter), stainless steel washers (1mm in thickness, 6.6 mm in internal diameter, and 15.8 mm in outer diameter) and a nut with different tightening torques. The bolt hole clearance is 80 μm, and is about 1.4% as seen in the aerospace bolted joint application [30] ~ [31]. To reduce the secondary bending moment in the fatigue testing, aluminum alloy plates of 4 mm in thickness were adhered at the grip sides of the bolted specimens with glue.

2.2 Fatigue testing

The fatigue testing was carried out under conditions of a frequency of 10 Hz, a stress ratio of 0.05 (a tension - tension type) and various stress amplitudes to obtain a S-N relation: a

relationship between the stress amplitude and the fatigue life (the number of cycles to failure). In the testing, the stress amplitude was obtained from the load amplitude divided by a net area of the cross section of 176 mm^2 (the whole area of the cross section – the area of the hole section). The fatigue testing of the bolt hole specimen was carried out by loading at a bolt hole edge through a steel pin (hereafter referred to as a pin loading). The effects of tightening torque on the fatigue life and failure modes were evaluated with bolt hole and bolted specimens at different stress amplitudes.

After the fatigue testing, the fracture surface and contact surfaces of the specimen were cleaned in an ultrasonic acetone bath, and then subjected to observation through scanning electron microscope (SEM).

2.3 Ultrasonic measurement

During fatigue testing, two types of ultrasonic measurements (the offline-measurement and the in-process measurement) were carried out by using a transducer generating a longitudinal wave of 20 MHz in frequency with a focal distance of 25.4 mm in water. The off-line measurement was carried out as shown in Fig. 2 (a). At required numbers of cycles in the fatigue testing, the specimen was taken out from the fatigue tester and set in a water tank for ultrasonic measurement with the immersion method. The ultrasonic wave was irradiated on the specimen surface at an angle of 30° from the plane normal to generate the SAW. The SAW propagated through contact surfaces to the bolt hole edge, and then detected by the transducer.

The in-process ultrasonic measurement was carried out by the local immersion method with a water bag [32] during the fatigue testing as shown in Fig. 2 (b). The transducer was encapsulated in the water bag and fixed with a rubber band as shown in the figure. The water bag used was made of latex rubber with a thickness of 69 μm. In the previous work [32], the longitudinal ultrasonic measurement was carried out by focusing the ultrasonic wave at the opposite side of the specimen, where as the surface acoustic wave measurement was carried out in the present work. At required numbers of cycles, the fatigue tester was kept at a mean load of the fatigue cycle, and the SAW measurement was carried out to obtain reflection echoes.

3. Results and discussions

3.1 Change in fatigue life with stress amplitude

Figure 3 shows the S-N relation of the bolt hole and the bolted specimens. The bolted specimen was fastened with a tightening torque of 4 to 6 Nm. In the case of the bolt hole specimen, a fatigue crack initiated at the edge of the bolt hole and propagated transversely to the loading direction as shown in Fig. 4 (a), and hereafter referred to as a mechanical fatigue crack. In the bolted specimen, a crack appeared near the bolt hole edge due to fretting damage and propagated transversely to the loading direction as shown in Fig. 4 (b), and hereafter referred to as a fretting crack. In the S-N diagram, the fatigue life of the bolt hole specimen was 20 to 50% lower than that of the bolted specimen in the measured range of the stress amplitude. The difference in the fatigue life is caused by difference in the loading condition. In the case of the bolt hole specimen, full load was carried to the hole edge through the bolt. However, in the case of the bolted specimen, the load was distributed over the contact surface by friction, which caused reduction of the stress concentration at the hole edge. Therefore the fatigue life of the bolted specimen took higher values than that of the bolt hole specimen.

Figure 5 shows SEM photographs of the abraded surface near the bolt hole of the bolted specimen. In this case, the fatigue testing was carried out at stress amplitude of 25 MPa and a tightening torque of 5 Nm, and the specimen was broken by the fretting fatigue cracking at the other plate. In the figure, there are two types of cracks: the mechanical fatigue crack from the bolt hole edge (a) and the fretting fatigue crack (b) near the bolt hole edge was observed.

3.2 Effect of tightening torque on fatigue life

A relationship between the tightening torque and the fatigue life of the bolted specimen was obtained at different stress amplitudes, as shown in Fig. 6. Three modes of failure are shown in the figure. In a range of smaller torques, the fatigue life of the bolted specimen increased with increasing tightening torque, and the mechanical fatigue failure occurred at the bolt hole edge as shown in Fig. 7 (a). When the tightening torque was increased further, the fretting wear failure occurred near the bolt hole due to the gross sliding of the specimen surfaces, and the fatigue life increased with increasing tightening torque as shown in Fig. 7 (b). At a higher range of tightening torque, the fatigue life decreased with

increasing tightening torque, and the fretting fatigue failure occurred near the bolt hole, as shown in Fig. 7 (c). Regardless of the stress amplitude, in the case of no tightening (i.e. the pin loading or 0 Nm), the fatigue life was shortest in the measured range of the tightening torque.

The change in the fatigue life and also the change in the failure mode of the bolted specimens from the mechanical fatigue failure to the fretting failure are discussed from the standpoint of loading conditions as follows.

A. Case of mechanical fatigue failure

At smaller tightening torque, the mechanical fatigue failure occurred. From the force balance as shown in Fig. 8,

$$P_{\max} = B_{\max} + F_f \ , \tag{1}$$

where $P_{\max}$ is the maximum of the load amplitude ΔP applied to the specimen, and $B_{\max}$ is the maximum of the load amplitude ΔB applied to the bolt hole. F_f is the frictional force at the contact area due to clamping of the material.

A relation between $B_{\max}$ and the maximum stress amplitude $\sigma_{\max}$ averaged through the thickness of the specimen is given by

$$B_{\max} = \sigma_{\max}\left(w - 2r\right)\, t \,, \tag{2}$$

where w and t are the width and the thickness of the plate, respectively, and r is the radius of the bolt hole. From the S-N curve in Fig. 3, a relation between the stress amplitude $\Delta\sigma$ and the fatigue life N_f is given by

$$\Delta\sigma = C\, N_f^{-m} \tag{3}$$

where m is the slope of the S-N curve for pin loading (the bolt hole specimen) in log-log scale and is about 0.274. With the relation between $\sigma_{\max}$ and $\Delta\sigma$, the maximum stress amplitude $\sigma_{\max}$ is given as function of fatigue life N_f as follows,

$$\sigma_{\max} = \frac{2}{1-R}\Delta\sigma = C'\, N_f^{-m} \ , \tag{4}$$

where R is stress ratio, C and C' are constants.

The frictional force F_f applied to the contact area is proportional to the clamping

force F_c by Amonton-Coulomb friction Law [10, 33], and, the clamping force F_c is proportional to the tightening torque T_b [34]. Therefore,

$$F_f = \mu F_c = \mu C'' T_b, \tag{5}$$

where μ is the coefficient of friction and C'' is constant.

Substituting equations (4) and (5) and into equation (1),

$$P_{\max} = C' N_f^{-m} \left(w - 2r\right) t + \mu C'' T_b. \tag{6}$$

By rearranging equation (6),

$$N_f = \frac{K}{\left(A - T_b\right)^{\frac{1}{m}}}, \tag{7}$$

where, $K = \left[C'\left(w - 2r\right) t / \mu C''\right]^{1/m}$ and $A = P_{\max} / \mu C''$.

The predicted value of the fatigue life given by equation (7) was plotted for different stress amplitude as the broken line in Fig. 6. The value of C' and m were calculated from the S-N curve of Fig. 3 for pin loading of the bolt hole specimen in log-log scale. The values of C'' was calculated from [9,34] and μ was assumed to be 0.6 (more than gloss sliding condition). From the figure, it is seen that the fatigue life N_f monotonically increases with the T_b.

B. Case of fretting wear failure

When the tightening torque increased further, larger portion of the load is transferred by the friction force F_f between the contact surfaces, and a smaller portion of the load is transmitted to the bolt hole by the bolt, and the stress at the bolt hole edge is reduced. This region is the transient one from the mechanical fatigue to the fretting fatigue and is also known as gross slip region of fretting. In this region, the change in the fatigue life with the increase in the torque can be also explained with equation (7). At a given stress amplitude with a lower tightening torque, the value of the friction force was insufficient to break the surface asperities, hence the failure occurs in the bolt hole edge. When the tightening torque is increased gradually, the sufficient friction force was generated due to decrease in the coefficient of friction to break the surface asperities to create the oxide debris [13]. This continuous ploughing of the surface asperities leads to the nucleation of the crack as well as roughened surfaces as seen in Fig. 7 (b). The fatigue life in this region increased with

increasing torque. This may be because embryo cracks are removed before they become critical size by the gross sliding of the specimen surfaces and also the increase in the clamping force reduces the crack propagation after nucleation. A critical tightening torque from the mechanical fatigue to the fretting failure decreased with the decreasing stress amplitude. For a given contact pressure, co-efficient friction decreases with decrease in the applied stress [13] ~ [14]. Hence the sufficient friction force was generated to break the surface asperities results in the higher rate of fretting failure at the lower stress amplitude.

The predicted value of the fatigue life for this case at the different level of stress amplitude as given from equation (7), was plotted as the broken line in Fig. 6. The values of the C' and m was calculated by the S-N curve for the bolted specimen in log-log scale from Fig. 3. The value of C'' was calculated from [9, 34] and μ was assumed 0.40 for the sliding condition of Al alloy [14]. From the figure, it is seen that the fatigue life N_f increases with the T_b.

C. Case of fretting fatigue failure

When the tightening torque increased further, the fretting fatigue failure occurred near the bolt hole. This region is often called as mixed stick-slip condition of fretting. The analytical modeling and expression of this region is explained by Szolwinski et. al. [4], as shown in Fig. 9, which states that the total maximum tangential stress at the edge of the contact area can be approximated as fretting contact stress and the applied bulk stress:

$$\sigma_{\max} = \sigma_{fretting} + \sigma_0 , \tag{8}$$

where $\sigma_{\max}$ is the tangential stress at the edge of contact, $\sigma_{fretting}$ is fretting contact stress and σ_0 is the applied bulk stress. And, $\sigma_{fretting}$ [4] is given by,

$$\sigma_{fretting} = 2 f_0 \sqrt{\frac{\mu Q}{F}} , \tag{9}$$

where F is the normal load, Q is the tangential load, μ is the coefficient of friction and f_0 is the maximum Hertzian contact pressure. The maximum stress at the fretted area is expressed by the following equation from (8) and (9).

$$\sigma_{\max} = 2 f_0 \sqrt{\frac{\mu Q}{F}} + \sigma_0 \quad , \tag{10}$$

The Smith-Matson-Topper equations (SWT) are used for the analysis of the fretting fatigue crack nucleation by many researchers [4, 36]. Since the propagation life of the fretting fatigue is small compared to nucleation [4], the analytical trend for the fretting fatigue failure was discussed with nucleation life. The relationship between total stress amplitude and the load cycles to the failure is described by SWT equations is given by

$$\sigma_{\max}\left(\frac{\Delta\varepsilon}{2}\right) = \frac{\left(\sigma_{f'}\right)^2}{E}\left(2N_f\right)^{2b} + \sigma_{f'}\varepsilon_{f'}\left(2N_f\right)^{b+c} \quad , \tag{11}$$

where $\Delta\varepsilon$ is the applied strain range, $\sigma_{f'}$ is the fatigue strength coefficient, b is the fatigue strength exponent, $\varepsilon_{f'}$ is the fatigue ductility coefficient, c is the fatigue ductility exponent and E is the modulus of elasticity. For the nominal elastic ranges and fully reversed loading cycle $\sigma_{\max}$ can be related to the strain amplitude [4]. So the SWT expression on the trailing edge of the contact becomes

$$\left(\frac{1-\upsilon^2}{E}\right)\left(\sigma_{\max}\right)^2 = \frac{\left(\sigma_{f'}\right)^2}{E}\left(2N_f\right)^{2b} + \sigma_{f'}\varepsilon_{f'}\left(2N_f\right)^{b+c}, \tag{12}$$

where υ is the Poisson's ratio. Substituting equation (10) in equation (12)

$$\left(\frac{1-\upsilon^2}{E}\right)\left(2 f_0 \sqrt{\frac{\mu Q}{F}} + \sigma_0\right)^2 = \frac{\left(\sigma_{f'}\right)^2}{E}\left(2N_f\right)^{2b} + \sigma_{f'}\varepsilon_{f'}\left(2N_f\right)^{b+c}. \tag{13}$$

The fretting crack nucleation can be estimated by iterative solution of the equation (13). The elastic constants used for the iteration summarized in Table 1 had also been used by Szolwinski et. al. [4] for the analysis of fretting crack nucleation of the aluminum alloy 2024-T351. The relation between clamping force and the tightening torque was calculated by using equation (5) and the maximum clamping stress f_0 was calculated by using equation [35]. The value of *Q/F* and μ were assumed to be 0.3 and 0.65, respectively for fretting

fatigue model of the aluminum alloy 2024-T351 [4]. The predicted value of the fretting fatigue crack nucleation at the different level of stress amplitude obtained by iteration of the equation (13) is plotted as the solid line in Fig. 6. As shown in the figure, the fatigue life N_f for the fretting fatigue decreases with the increase in the T_b.

The fretting contact provides a stress concentration σ_{max} / σ_0 at the contact surface. This stress concentration reduces the fatigue life of the material. Hence for the bolted specimen, when the contact load, namely tightening torque was increased further, a larger portion of the load is transferred by friction force between the contact surfaces where as the bolt transmit only a smaller portion of the load to the bolt hole. This results in the decrease in the stresses at the bolt hole edge and increase in the frictional stress amplitude [16]. The increase in the frictional stress amplitude increases stress concentration at the fretted area and hence fatigue life decreases. Many studies and experimental result show that the fretting fatigue life decreases with the increase in the clamping force [12] ~ [14] and [16], namely with the increase in the tightening torque. This stress concentration leads to the decrease in the cycle number of crack initiation in the fatigue process and the acceleration of the crack growth by fretting.

C. Change in the failure mode with tightening torque

From the above discussion, it is found when the tightening torque T_b is relatively lower, the mechanical fatigue failure is dominant, and the fatigue life is increased with increasing tightening torque. When the tightening torque T_b is higher, to the contrary, the fretting failure is dominant and the fatigue life is increased with increasing tightening torque in fretting wear region and decreased with increasing tightening torque in fretting fatigue region.

3.3 Intensity distribution of SAW

At different numbers of the fatigue cycles, the off-line SAW measurement was carried out. Figure 10 shows a typical distribution of the SAW along the specimen surface. In this case, the fatigue testing was carried out under conditions: a tightening torque of 4 to 6 Nm and stress amplitude of 25 MPa, and the fretting fatigue crack appeared and propagated. At an initial stage (N = 0), echoes reflected from the specimen edge (E), the squeezing edge (S) and the hole edge (Bh) were observed in the intensity distribution of the SAW. At

170,000 cycles, an echo C was detected ahead of the bolt hole edge. A distance between the echo and the bolt hole edge was evaluated to be about 1.9 mm by using a velocity of 3030 m/s (measured in the preliminary experiment). At 180,000 cycles, the specimen was unfastened for observation. As shown in Fig. 11, a crack of 6mm in length was observed at a position 1.8 mm from the bolt hole edge, which was in good agreement with a crack position evaluated from the SAW measurement.

Then, the in-process SAW measurement was carried out in the fatigue testing under the same conditions as the off-line measurement. As shown in Fig. 12, at an initial stage (N = 0), echoes reflected from the specimen edge (E), the squeezing edge (S) and the hole edge (Bh) were observed. The reflection from the specimen edge (E) and the squeezing edge (S) decreased with the increase in the number of fatigue cycle. This may be due to occurrence of the slipping during the fatigue process. The change in the intensity of the scattering wave ahead of the reflection Bh was observed till 120,000 cycles due to fretting process. Then, at 1.8 mm from the bolt hole, an echo C appeared at a fatigue life cycle of around 125,000 cycles. The intensity of the reflection C increased gradually with the propagation of the crack. Though the SAW was propagated on the surface of the lower plate of the bolted specimen, the fracture occurred at the upper plate at 183,200 cycles. Then the specimen was unfastened and the photograph of the fretting surface was taken. A surface crack of 12 mm in length was observed at a position of 1.7 mm ahead of the bolt hole edge as shown in Fig. 13, a position of which is coincident with the edge of the fretted area around the bolt hole. The measured crack position was in good agreement with one estimated from the SAW distribution. Then, the offline SAW measurement was also carried out for this specimen after the fatigue testing. Figure 14 shows a typical distribution of the SAW along the specimen surface. The reflection C from the crack ahead of the bolt hole edge reflection Bh was observed clearly during the measurement. The evaluated crack position from the offline SAW measurement was in good agreement with one estimated from the in-process SAW distribution. In one of the specimen, the specimen edge (E) was polished and rounded to observe the change in the intensity of the reflection from the bolt hole edge (Bh). But no major change was observed in the intensity of Bh except the decrease in the intensity of the reflection from E.

The crack position was evaluated from the SAW measurement for bolted specimens fastened with different torques, and compared with the measurement as shown in Fig. 15.

The position of the crack estimated from the SAW measurement was in good agreement with that measured on the specimen surface.

4. Conclusion

The fatigue testing was carried out with bolted specimens and bolt hole specimens of A2024-T3 alloy under different tightening torques. The fatigue life of the bolted specimen increased with increasing tightening torque in the lower range of tightening torque, and the failure occurred at the bolt hole edge. At the higher range of torque, fretting wear and fretting fatigue was observed and the fractured occurred near the bolt hole. In the fretting wear region, the fatigue life increased with increasing torque where as in the fretting fatigue region, the fatigue life decreased with increasing torque. These trends were compared with the analytical modeling.

The surface acoustic wave measurement was also carried out by using the water bag during fatigue testing of the bolted specimen, and the reflection echoes from the specimen edge, squeezing edge, bolt hole edge and the fretting fatigue crack were obtained. With the SAW measurement, fretting fatigue crack of about 12 mm in length was detected in the fatigue process. The intensity of the reflection from the fretting crack increased gradually with the number of fatigue cycles. The position of the crack estimated from the SAW measurement was in good agreement with the measured one.

The ultrasonic measurement by using the water bag in the present work demonstrates the potential of the surface acoustic wave as a tool for nondestructive detection of the fretting fatigue crack at the interface of the bolted joint under the fastened condition. The limitation of this ultrasonic measurement with the water bag is appropriate only for the flat object.

Acknowledgements

The authors would like to thank Dr. K. Kageyama, Associate Professor, Saitama University, for his useful discussion. The authors would also like to thank Mr. Y. Kawada, Technical Associate of Saitama University, for his help in specimen preparation. The present work was carried out in part under the financial support of Grant for Research Project in 2006 (Project no.A06-631) of Saitama University.

References

1. D. Steadman and R. Ramakrishnan, Simulation of multiple site damage growth, 9th joint FAA/ DoD/NASA Aging aircraft Conf., Atlanta GA, March (2006).
2. A report of the Airworthiness Assurance Working Groups, Widespread fatigue damage bridging tasks, Multiple element damage, July 23 (2003), 15-57.
3. H. Terada, Structural fatigue and joint degradation, Int. J. Fatigue, 23 (2001) S21-S30.
4. M. P. Szolwinski and T.N. Farris, Observation, analysis and prediction of fretting fatigue in 2024-T351 aluminum alloy, Wear, 221 (1998), 24-36.
5. S. R. Shinde and D. W. Hoeppner, Fretting fatigue behaviour in 7075-T6 aluminum alloy, Wear, 261 (2006), 426-434.
6. C.B. Elliott III and D. W. Hoeppner, The importance of wear and corrosion on the fretting fatigue behavior of two aluminum alloys, Wear 236 (1999), 128-133.
7. Y.K. Chen, L. Han, A. Chrysanthou and J.M. O'Sullivan, Fretting wear in Self piercing riveted aluminum alloy sheet, Wear 255 (2003), 1463-1470.
8. S. Munoz, H. Proudhon, J. Dominguez and S. Fouvry, Prediction of the crack extension under fretting wear loading conditions, Int. J. Fatigue, 28 (2006) 1769-1779.
9. J. M. Mınguez and J. Vogwell, Effect of torque tightening on the fatigue strength of bolted joints, Eng. Failure Analysis, 13 (2006), 1410-1421.
10. J. Dominguez, Cyclic variations in friction forces and contact stress during fretting fatigue, Wear 218, (1998), 43-53.
11. R.C. Alderliesten, M. Hagenbeek, J. J. Homan, P.A. Hooijmeijer, T. J. De Vries and C.A.J.R. Vermeeren, Fatigue and damage tolerence of glare, Appl. Comp. Materi., 10 (2003), 223-242.
12. K. Nakazawa, N. Maruyama and T. Hanawa, Effect of contact pressure on fretting fatigue of austenitic stainless steel, Tribology Int., 36 (2003), 79-85.
13. N.K.R. Naidu and S.G.S. Raman, Effect of contact pressure on fretting fatigue behavior of Al-Mg-Si alloy AA6061, Int. J. Fatigue, 27 (2005) 283-291.
14. P.R. Arora, M.S.D.Jacob, M.S. Salit, E.M. Ahmed, M.Saleem,,P. Edi, Experimental evaluation of fretting fatigue test apparatus, Int. J. Fatigue, 29 (2007) 941-952.
16. K. Nishioka and K. Hirakawa, Fundamental investigation of fretting fatigue, Bull Jpn. Soc. Mech. Engr., 15 (1972), 135-144.
17. S. Adibnazari and D. W. Hoeppner, A fretting fatigue normal pressure threshold

concept, Wear, 160 (1993), 33-35.

18. R. Osegueda, V. Kreinovich, S. Nazarian and E. Roldan, Detection of cracks at rivet hole in thin plates using lamb wave scanning, The university of Texas at El Paso, El Paso, Texas 79968.
19. Z. Chang and A. Mal, Scattering of Lamb waves from a rivet hole with edge cracks, Mech. Mater., 31 (1999), 197-204.
20. B. Mi, J. E. Micheals and T. E. Michaels, An ultrasonic method for dynamic monitoring of Fatigue crack initiation and growth, J. Acoust, Soc. America, 119 (2006), 74-85.
21. J. E. Micheals, T. E. Michaels and B. Mi, An ultrasonic Angle beam method for in situ sizing of fastener hole, J. Nondest. Eval., 25(1) (2006), 3-16.
22. C. P. Chiou, F. J. Martegetan and J.H. Bose, Ultrasonic detection of cracks below bolts in aircraft skin, QNDE, 10B (1991), 1891-1897.
23. M.A.S. Akanda and M. Saka, Ultrasonic shear wave technique for sensitive detection and sizing of small closed cracks, JSME Int. J., Seri., A 45(2) 2002, 252-261.
24. M. Saka and M.A.S. Akanda, Ultrasonic measurement of crack depth crack opening stress intensity factor under a no load condition, J. of Nondest. Eval., 23(2) (2004), 49-63.
25. M.A.S. Akanda and M. Saka, Relation between closure stress of small fatigue crack and ultrasonic response, J. of Nondest. Eval., 23(2) (2004), 37-47
26. S.R. Ahmed and M. Saka, Influence of wall thickness on the ultrasonic evaluation of small closed surface cracks and quantitative NDE, J. of Nondest. Eval., 21(1) (2002), 37-47
27. J.-Y. Kim and S.I. Rokhlin, Surface acoustic wave measurements of small fatigue cracks initiated from a surface cavity, Int. J. Solids and Struct., 39 (2002), 1487–1504.
28. Y.H. Kim, S.-J. Song, D.H. Bae and S.-D. Kwon, Assessment of material degradation due to corrosion-fatigue using a backscattered Rayleigh surface wave, Ultrasonics, 42 (2004), 545–550.
29. D.A. Cook and Y.H. Berthelot, Detection of small surface breaking crack in steel using scattering of Rayleigh waves, NDT & E Int., 34 (2001), 483-492.
30. V.P. Lawlor, M.A. McCarthy and W.F. Stanley, An experimental study of bolt hole clearance effects in the double-lap, multi-bolt composite joints, Comp. Structure, 71

(2005), 176-190.

31. M.A. McCarthy, V.P. Lawlor, W.F. Stanley and C.T. McCarthy, Bolt hole clearance effects and strength criteria in single-bolt, single-lap, composite bolted joints, Comp. Sci. and Tech., 62 (2002), 1415-1431.
32. X. Min and H. Kato, Change in ultrasonic parameters with loading/unloading process in cyclic loading of aluminum alloy, Mater. Sci. and Eng., A 372 (1-2) (2004), 269-277.
33. S. Suresh, *Fatigue of Materials*, Second Edition, CambridgeUniversity Press, UK (1998), 466-473.
34. J. E. Shigley and C. R. Mischke, *Mechanical Engineering Design*, Fifth Edition, McGraw-Hill Book Co., Singapore (1989), 345-346.
35. M. P. Szolwinski and T.N. Farris, Mechanics of fretting fatigue crack formation, Wear, 221 (1998), 24-36
36. C.D. Lykins, S. Mall and V. Jain, An evaluation parameter for predicting fretting fatigue crack initiation, Int. J. Fatigue, 22 (2000) 706-716

Figure caption

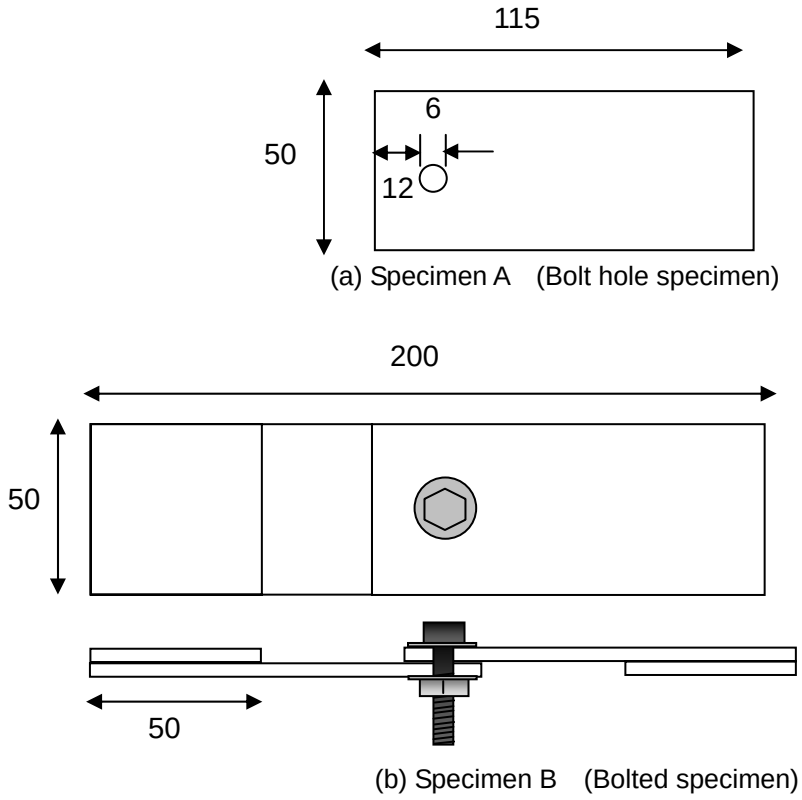

Fig. 1 Shape and dimensions of specimens for fatigue testing.

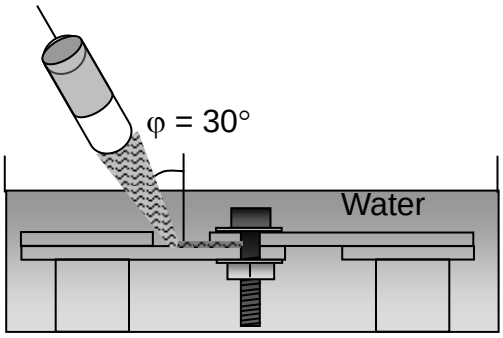

(a) Off-line SAW measurement with immersion method

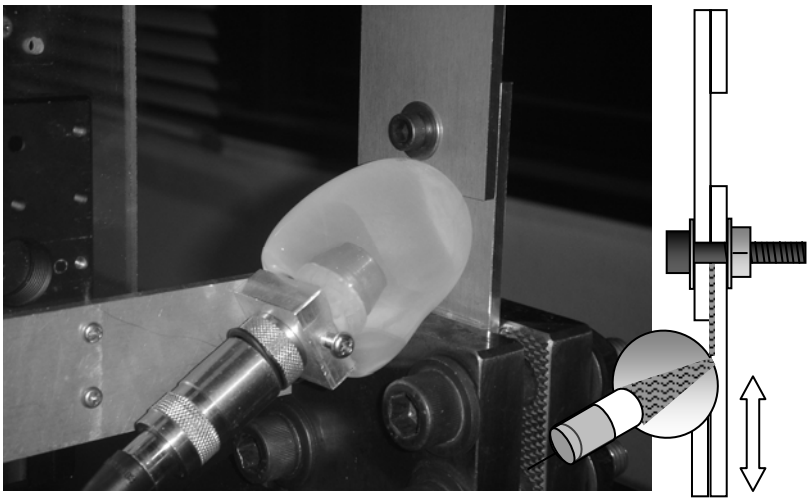

(b) In-process SAW measurement with local immersion method with water bag method

Fig. 2 Setup for ultrasonic measurement of SAW.

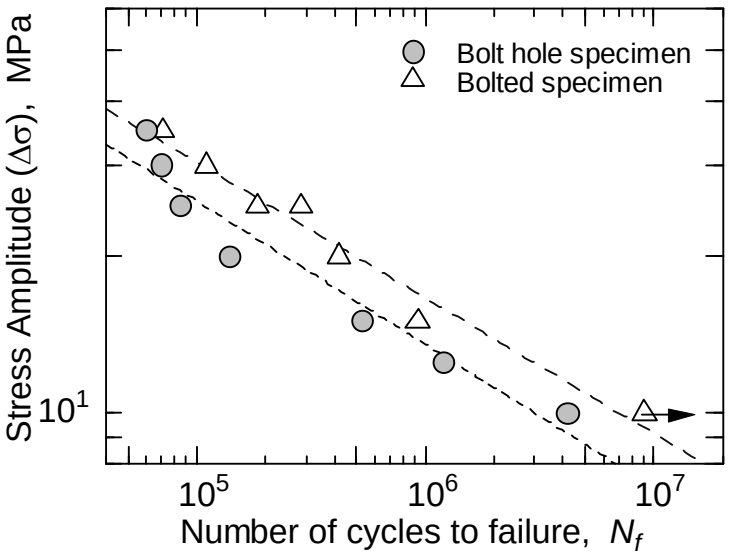

Fig. 3 Stress amplitude vs number of fatigue cycles to failure of bolt hole specimen and bolted specimen in log – log scale. (arrow indicates specimen was not fractured)

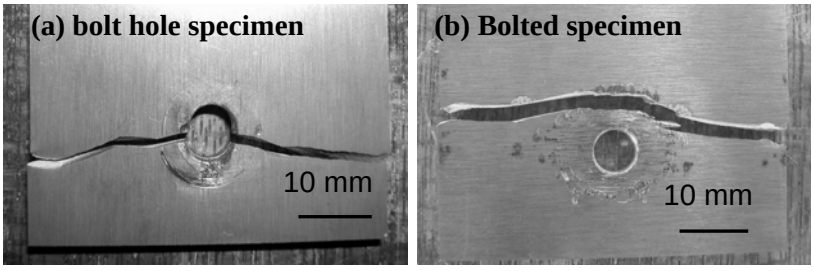

Fig. 4 Difference in crack propagation due to different loading in fatigue testing.

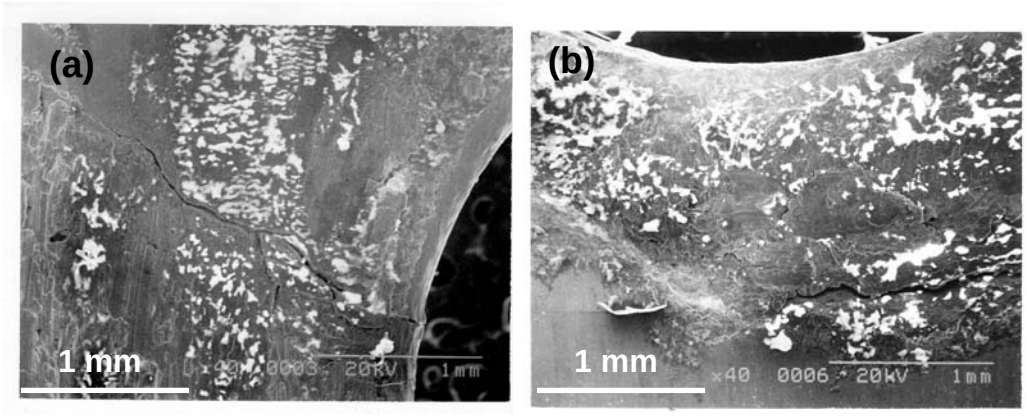

Fig. 5 SEM photographs of contact surface of bolted specimen. (a) mechanical fatigue crack, (b) fretting fatigue crack.

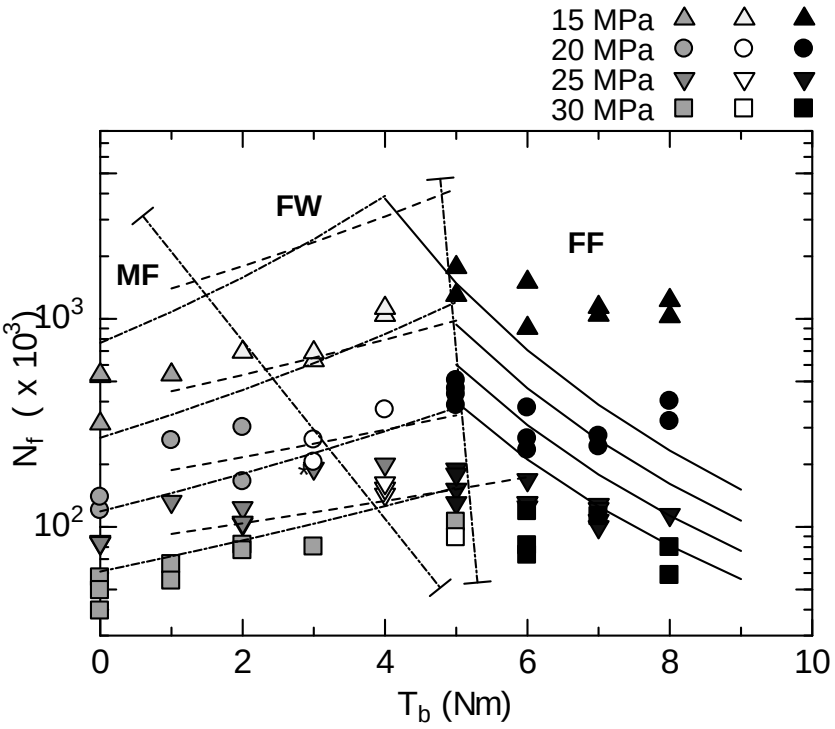

Fig. 6 Change in fatigue life N_f with tightening torque T_b of bolted specimen at a different stress amplitude. MF, FW and FF are Mechanical fatigue, Fretting wear and Fretting fatigue failure, respectively. * bolt broke just before specimen

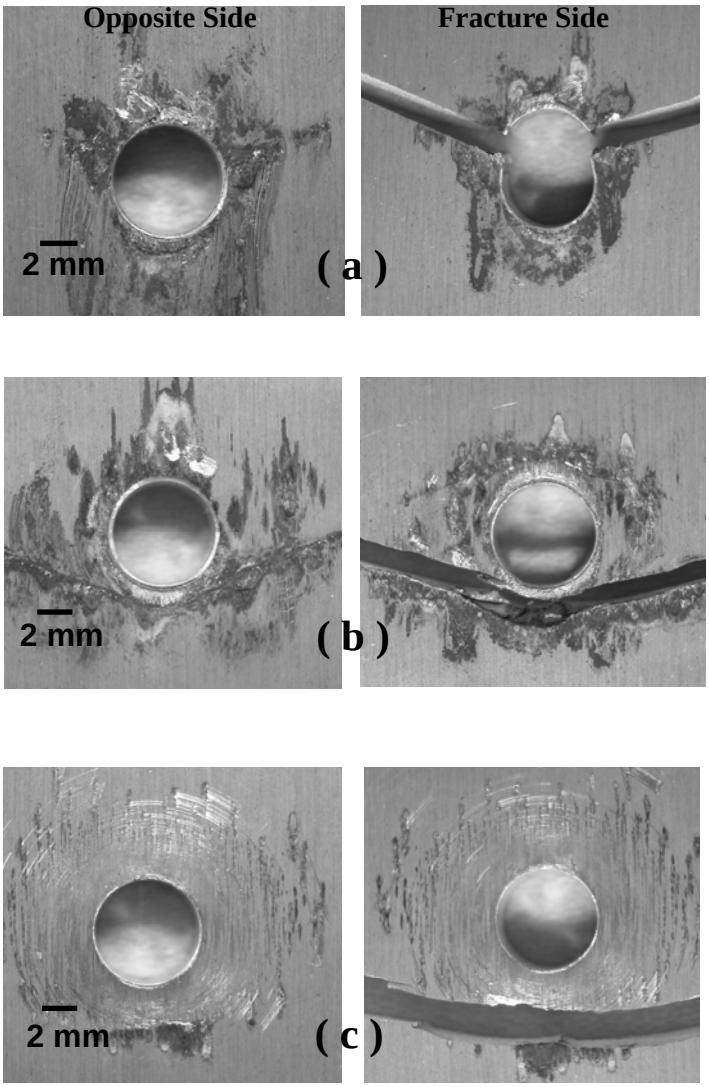

Fig. 7 Difference in crack propagation due to different tightening condition in fatigue testing at the stress amplitude of 15 MPa. (a) Mechanical fatigue at1 Nm (b) Fretting wear at 3Nm (c) Fretting fatigue at 8 Nm

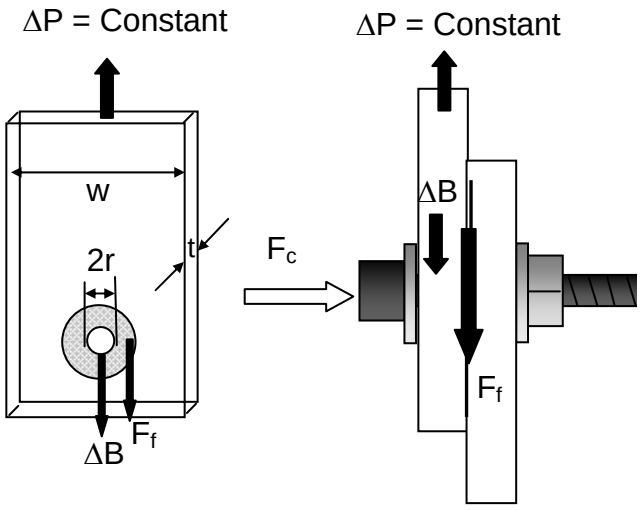

Force balance in bolted specimen

Fig. 8 Analytic model for mechanical fatigue failure at lower tightening torques.

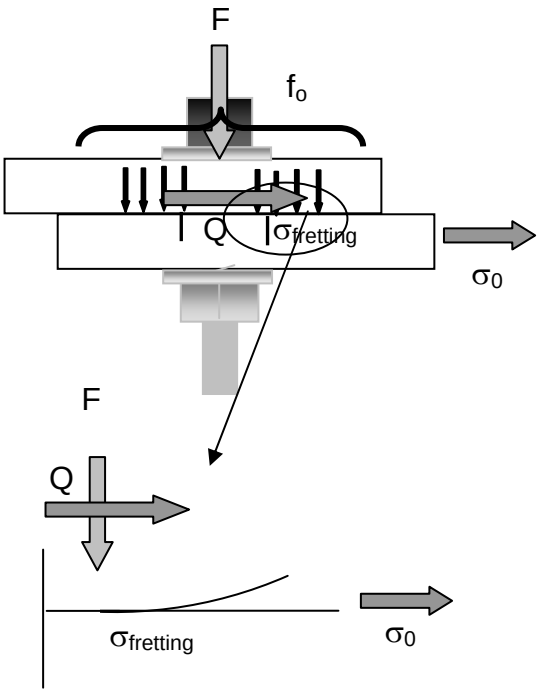

Fig. 9 Analytic model for fretting fatigue failure at higher tightening torques.

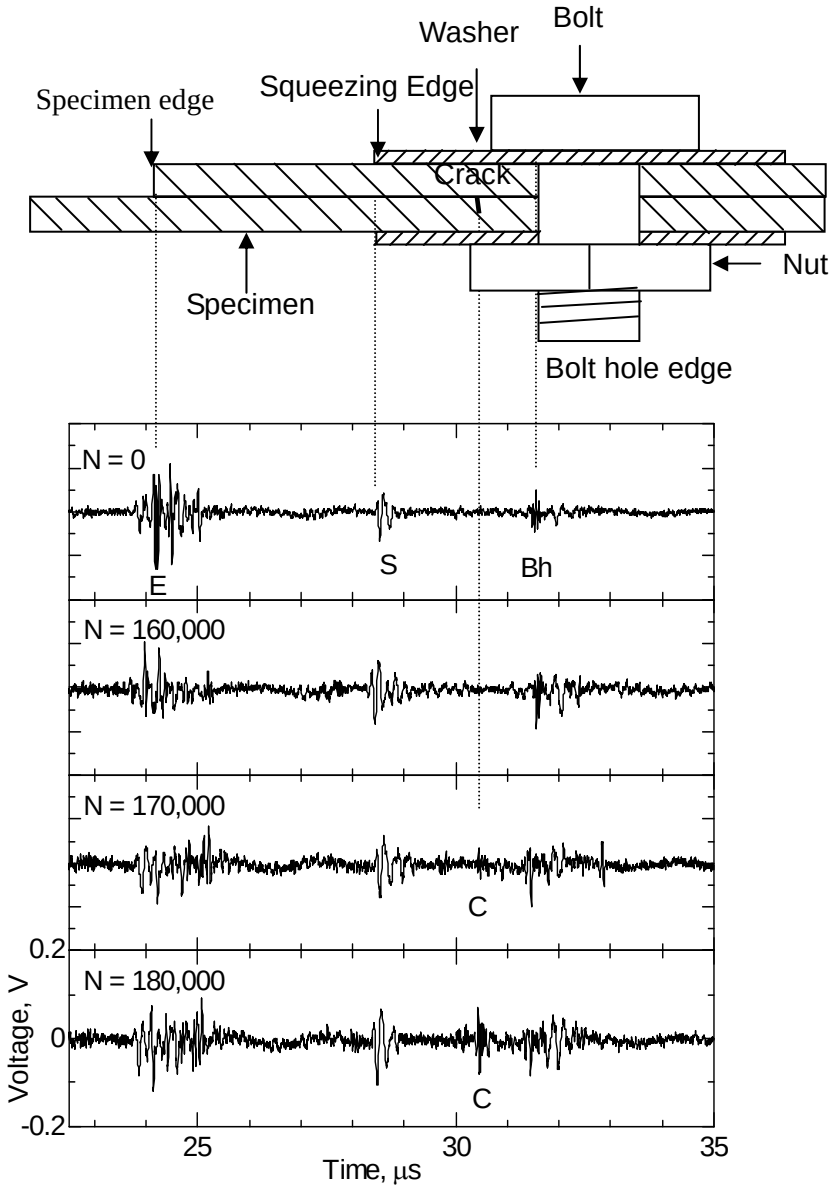

Fig. 10 SAW distribution obtained by off-line measurement at different loading cycles N.

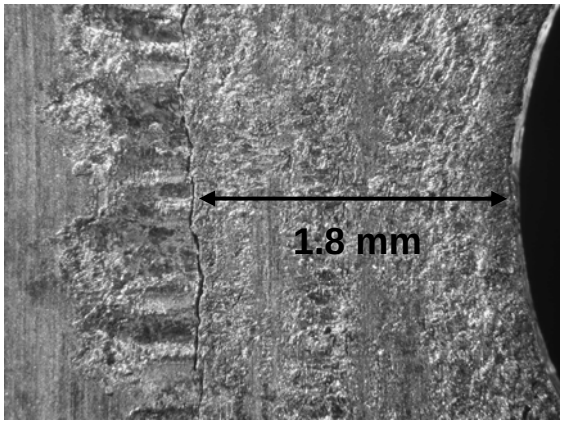

Fig. 11 Fretting fatigue crack appeared on contact surface of bolted specimen after fatigue testing.

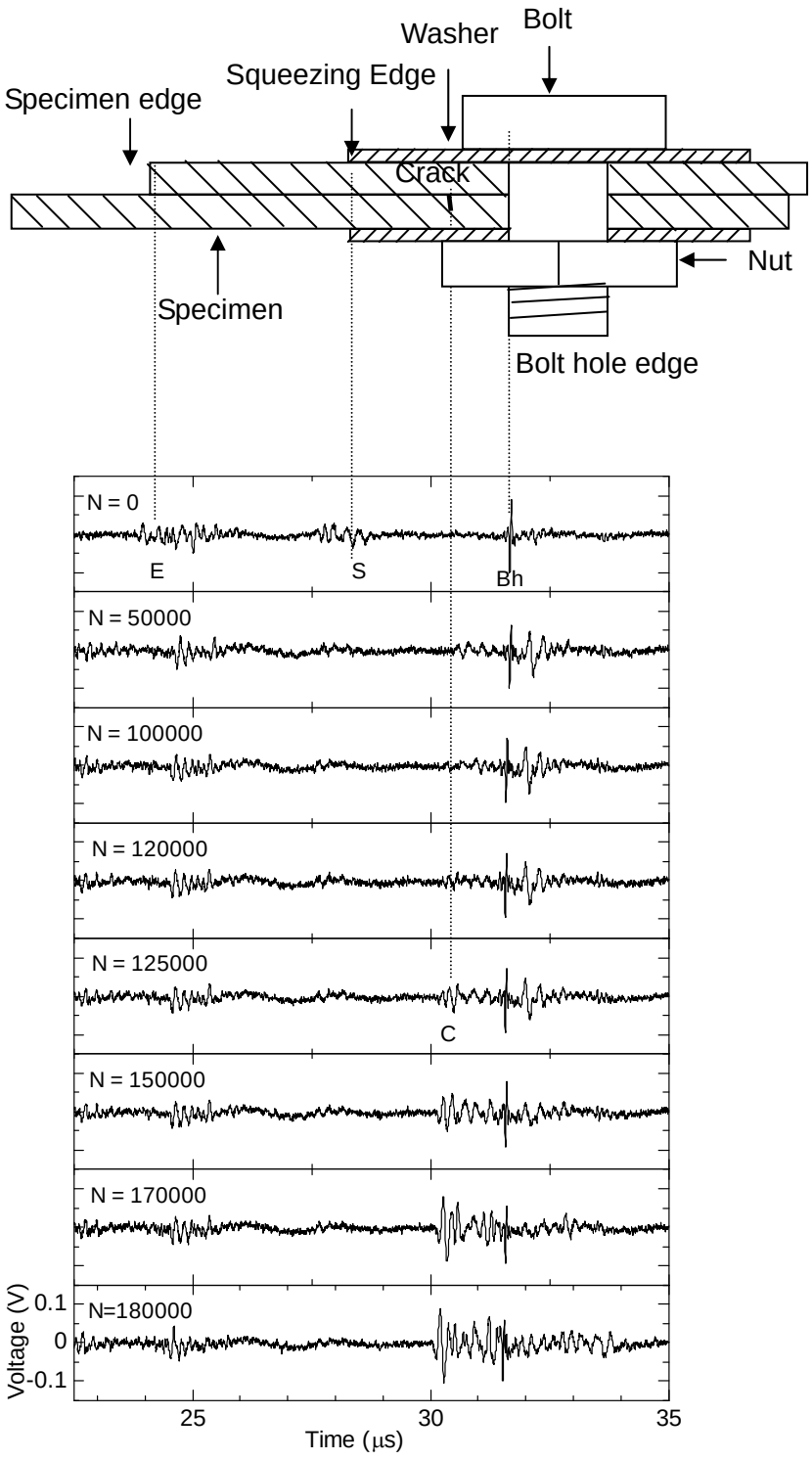

Fig. 12 SAW distribution obtained by in-process measurement at different cycles N.

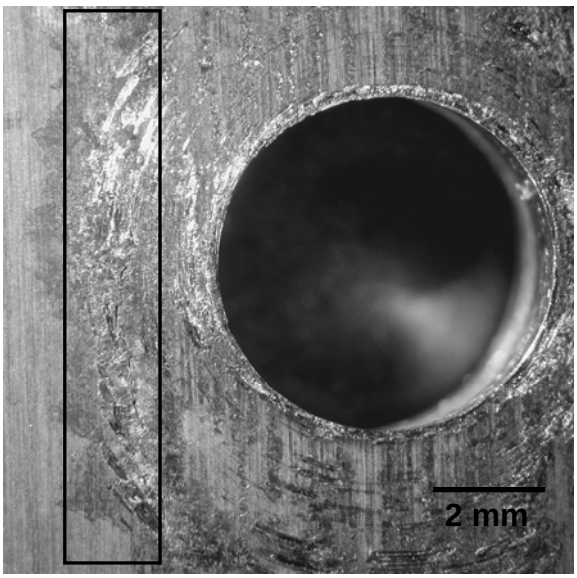

Fig. 13 Fretting fatigue cracks on the contact surface after fatigue testing.

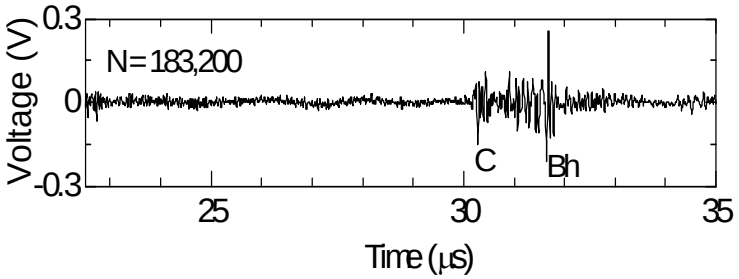

Fig. 14 SAW distribution obtained by off-line measurement at N =183,200.

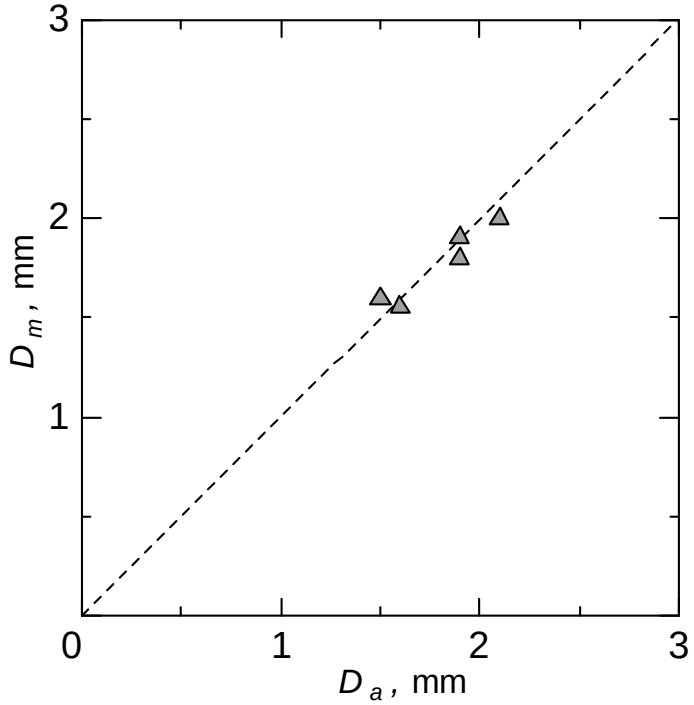

Fig. 15 Comparison of crack distance from bolt hole edge measured from SAW distribution D_m with that measured on specimen surface D_a.

Table 1. A summary of 2024- T 351 aluminum alloy material constants used in the fretting fatigue crack analysis [4]

σ_f	Fatigue strength co-efficient	714 MPa
B	Fatigue strength exponent	-0.078
ε_f	Fatigue ductility co-efficient	0.166
C	Fatigue ductility exponent	-0.538
E	Young's modulus	74.1 MPa
ν	Poisson's ratio	0.33